Hindawi Publishing Corporation
Advances in Materials Science and Engineering
Volume 2015, Article ID 909523, 8 pages
http://dx.doi.org/10.1155/2015/909523

Research Article

Feasible Time Evolution Model That Predicts Breakdown in Thin SiO_2 Films within Unstressed Interval after Constant-Current Stress

Yasuhisa Omura

ORDIST, Graduate School of Science and Engineering, Kansai University, 3-3-35 Yamate-cho, Suita, Osaka 564-8680, Japan

Correspondence should be addressed to Yasuhisa Omura; omuray@kansai-u.ac.jp

Received 17 December 2014; Revised 5 February 2015; Accepted 6 February 2015

Academic Editor: Filippo Giannazzo

This paper proposes a poststress time evolution model for sub-10-nm thick SiO_2 films for degradation prediction and the extraction of trap-related parameters. The model is based on the understanding that the degradation in thin SiO_2 films continues within the unstressed interval. The phenomenon is captured by an analytical expression that indicates that the time evolution of SiO_2 film degradation roughly consists of two stages and that the degradation is more likely to occur if water molecules are present. It is demonstrated that the simple analytical model successfully reproduces measured results. It is also suggested that the degradation process considered here is related to oxygen diffusion in the resistive transition process.

1. Introduction

It is well known that stress-induced leakage current (SILC) is observed in sub-10-nm thick SiO_2 films after the application of constant-current stress (CCS) or constant-voltage stress (CVS) [1, 2]. In this thickness range (4~8 nm), oxide breakdown and oxide degradation are among the most important factors influencing reliability. SILC observations suggest that traps are created in the SiO_2 film over time [1, 2]. The SILC of tunnel oxide films is, at present, the major factor impeding the downscaling of nonvolatile memory devices because a high oxide field is needed if the film is to permit data to be written and read reliably [3]. According to the ITRS Roadmap, the tunnel oxide film thickness (T_{ox}) should be held to around 6 to 7 nm [4]. However, it is inevitable that sub-6-nm thick SiO_2 films will be needed given the continuing decrease in supply voltage. Furthermore, recent works have reported that SILC can be related to the increase in neutral electron traps generated by hot electrons [5], and dielectric breakdown occurs as soon as a certain critical density of neutral electron traps in the oxide is reached [6, 7]. Although an electrical stress experiment has already been performed to investigate the time evolution of SILC events, the importance of the unstressed interval has not been well considered [5].

Recently, the author proposed a physical model of the time evolution of SILC events within the unstressed interval by characterizing the post-SILC degradation of SiO_2 films [8]; the diffusion of H_2 and H_2O molecules induces many Si–OH bonds (neutral E' center) which influence electron conduction, after the unstressed time interval ($T_{interval}$), through the neutral electron traps, such as Si– and SiO–, which are generated by the electrical stress [8]. However, the model was rather complex since it took account of the many chemical processes possible.

Silicate films and transition metal-oxide films are also attracting attention due to the resistive transition phenomenon [9–11] which should yield the creation of new nonvolatile memory structures [12, 13]. Therefore, a full characterization of silicon oxide film is very important in deeply understanding the mechanism of resistive transition and the resulting performance degradation.

This paper develops a feasible time evolution model to predict the breakdown due to the stress-relaxation process during the unstressed period by analyzing the degradation of metal-oxide-semiconductor (MOS) capacitors with 5.2-nm thick SiO_2 films. The paper addresses extra active trap creation within the unstressed interval. Possible theoretical models are proposed and compared to measured results;

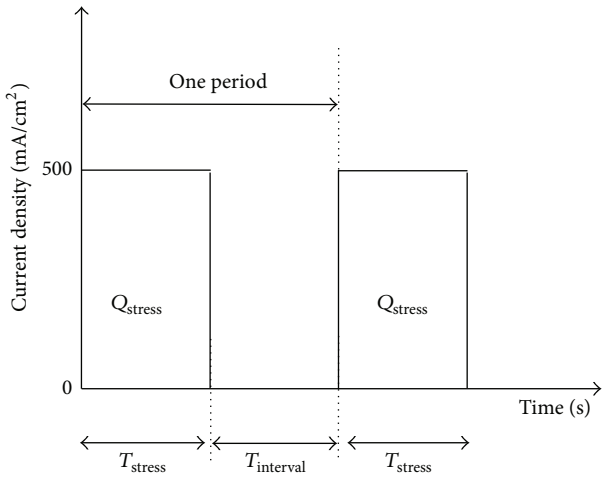

FIGURE 1: Experimental procedure of constant-current stress application. *Every* CCS condition is 500 mA/cm^2 *in all experiments.* Q_{stress} is 6 C/cm^2 or 12 C/cm^2.

they suggest that degradation proceeds in two stages, and several important physical parameters are extracted from the experiment's results. Finally, we address oxygen diffusion in the resistive switching process of SiO_2 film [9, 10].

2. Device Fabrication and Stress Method

The MOS capacitor (T_{ox} = 5.2 nm) examined here has an *n*-type poly-Si/SiO_2/Si substrate stack structure; its *n*-type (001) silicon substrate has resistivity of 4 Ωcm. The SiO_2 film is fabricated at 950 C by the rapid thermal oxidation technique, followed by the chemical vapor deposition of phosphorus-doped amorphous silicon [14]. Wet etching is used to pattern the poly-Si film into a gate electrode (150 μm × 200 μm) to minimize processing damage.

In the present experiment, a short electrical stress was imposed on the MOS capacitor as shown in Figure 1. The CCS condition was 500 mA/cm^2 and was applied to the SiO_2 film until a fixed number of electrons were injected. The density of electronic charge (Q_{stress}) injected during one CCS cycle was either 6 C/cm^2 or 12 C/cm^2. After one CCS cycle, the gate electrode was held open for various periods ($T_{interval}$) at room temperature. The current-voltage (*I-V*) characteristics of the post-CCS SiO_2 film were at first evaluated just after the CCS cycle in order to observe how the SILC develops; $I_{stress}(T_{stress})$ was evaluated, where T_{stress} denotes the stress time. After the unstressed interval ($T_{interval}$), *I-V* characteristics were again measured in order to confirm subsequent SILC development; $I_{stress}(T_{stress} + T_{interval})$ was evaluated. Plotting the curve of $I_{stress}(T_{stress}+T_{interval})/I_{stress}(T_{stress})$ as a function of gate voltage (V_g) yields a specific peak $I_{stress}(T_{stress} + T_{interval})/I_{stress}(T_{stress})$ at V_g of 3.6 V (not shown here) [8, 15]. Accordingly, we use this value of $I_{stress}(T_{stress} + T_{interval})$ as representative of SILC hereafter.

In the following section, the time-to-breakdown (T_{bd}) is taken to be the integration of stress time (T_{stress}) and the hard breakdown (HBD) event is defined as the time at which the gate voltage stepped down by half during the CCS test. In order to determine the Weibull slope, β, at least 50 capacitors were measured for each case and the variation, taken to be the difference between the highest and the lowest confidence bounds of the β value, is plotted as a function of sample size by using the maximum likelihood estimation at the 95% confidence level.

3. Results and Discussion

3.1. Statistical Consideration of T_{bd}. In conventional CCS tests, the electrical stress is continuously imposed until hard breakdown occurs. In the present experiment, however, the electrical stress is periodically imposed on the MOS capacitor as shown in Figure 1. After one cycle of CCS, the gate electrode is held open for one week at room temperature. This sequence was repeated until the MOS capacitor exhibited HBD; hereafter we call this "periodic stress method with unstressed interval (PSMI)". The proposed method is different from the conventional unipolar-pulsed stress [16, 17]; the duty cycle is 50% in the conventional experiment, while it is much smaller than 50% and the frequency is much less than 1 Hz in the present one.

Weibull distributions of T_{bd} are shown in Figure 2. Three different current stress categories are compared; the first one is the conventional CCS *without any unstressed interval*, the second one is the PSMI with Q_{stress} of 6 C/cm^2 *and one week unstressed interval*, and the third one is the PSMI with Q_{stress} of 12 C/cm^2 *and one week unstressed interval.* In Figure 2, the PSMI without net $T_{interval}$ is used to provide a baseline for the basic periodic CCS method. In the PSMI method without any unstressed interval, the CCS (Q_{stress} = 6 C/cm^2 or 12 C/cm^2) was repeated without any unstressed interval. It should also be noted that all T_{bd} plots are identical to each other in Figure 2. Consequently, it can be concluded that the conventional CCS method and the PSMI without net $T_{interval}$ exhibit no substantial difference.

Next, we investigated how the finite value of $T_{interval}$ of PSMI influenced oxide breakdown. Weibull distributions of T_{bd} under PSMI with Q_{stress} of 12 C/cm^2 *and one-week unstressed interval* are shown in Figure 3(a), where T_{bd} distributions with and without net $T_{interval}$ are shown for comparison. The two Weibull distributions of T_{bd} in Figure 3(a) cross in the center of the distribution, and the slopes (β) are very different. The Weibull slope for the PSMI *with the one-week unstressed interval* is steeper than that without the net interval. This suggests that uniform degradation occurs inside the SiO_2 film over the one-week unstressed interval because it is expected that the initial total energy accumulated at the molecule by the electrical stress yields many traps during the unstressed time interval as discussed in the following section; this degradation process should accelerate the breakdown and then the Weibull slope is steeper than that in the conventional CCS. It can be considered that the traps created in the active CCS period (T_{stress}) generate some extra traps around themselves in the $T_{interval}$. This would be possible when defects created by the CCS relax their structural strain.

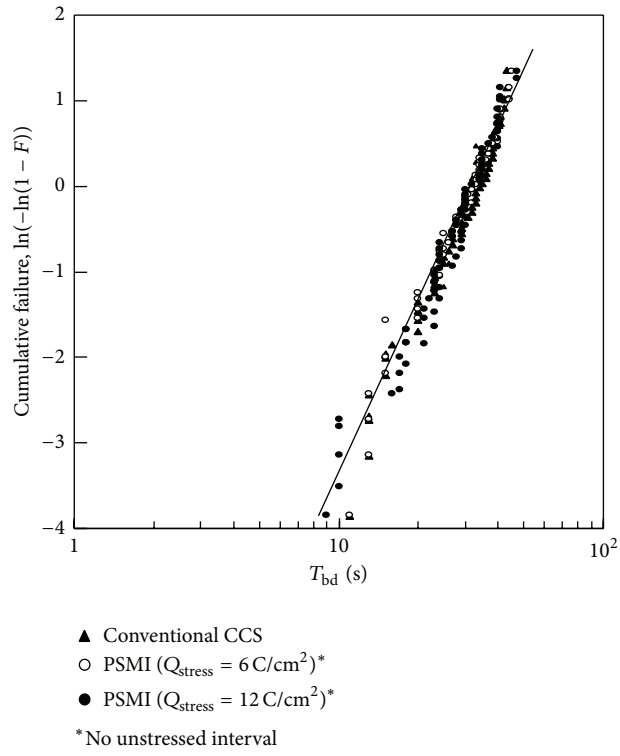

FIGURE 2: Distributions of T_{bd} for various stress conditions. Triangles show the T_{bd} distribution for the conventional CCS *without any unstressed interval*. Open and closed circles show T_{bd} distributions for the PSMIs with Q_{stress} of 6 C/cm^2 and Q_{stress} of 12 C/cm^2 with no unstressed interval, respectively.

Therefore, note that the poststress spatial extension of CCS-induced traps is a secondary result of failure events around initial trap sites [18]. Although the reason, why the average t_{bd} value for the PMSI experiment is larger than that for the conventional CCS experiment is not clear, I guess that the PSMI may lead to a certain degradation phase different from the conventional degradation that yields the SILC [8].

Weibull distributions of T_{bd} under PSMI with Q_{stress} of 6 C/cm^2 *and the one-week unstressed interval* are shown in Figure 3(b), where T_{bd} distributions with and without net $T_{interval}$ are shown for comparison. The two Weibull distributions of T_{bd} in Figure 3(b) are parallel to each other; the slopes are almost identical to those in Figure 2; the Weibull distribution for PSMI *with the one-week unstressed interval* is shifted to the left. This suggests that *the one-week unstressed interval* advances the percolation process of traps inside the SiO_2 film. In other words, it can be considered that the area of trap states created in the active CCS period (T_{stress}) expands due to some additional mechanisms [18] and generates some extra traps around themselves within $T_{interval}$. It is anticipated that the spatial expansion of trap states reduced the average value of T_{bd} for the PSMI method because it should accelerate the percolation process of traps. This is possible when the structural strain induced by defects created by CCS relaxes; this is also a secondary result of failure events around initial trap sites [18].

As a result, the above results strongly suggest that the generation of extra traps expands in three dimensions. Therefore, it is anticipated that such phenomena observed in this paper are related to those observed in [18]. However, we cannot conclude that the degradation observed in this study is the protrusion in the SiO_2 film[19].

3.2. Time Evolution of SILC Component. We evaluated the time evolution of the increase in gate current after *one CCS cycle* [8]; the increase $\Delta I(T_{stress} + T_{interval})$ is defined by $I_{stress}(T_{stress} + T_{interval}) - I_{stress}(T_{stress})$, where T_{stress} is 12 s for Q_{stress} = 6 C/cm^2 or 24 s for Q_{stress} = 12 C/cm^2. In order to determine the normalized increase, $\Delta I(T_{stress} + T_{interval})/I_{stress}(T_{stress})$, at least 5 capacitors were measured using various values of $T_{interval}$. In each case, the experimental error was 4.6% for Q_{stress} = 6 C/cm^2 and 3.5% for Q_{stress} = 12 C/cm^2; these error values are within the allowable margin. It has already been described that the increase in SILC is directly related to the increase in the number of traps yielding SILC under the stress applied [5]. Actually, the number of neutral traps generated is proportional to the injected charge, and the increase in SILC is proportional to the number of neutral traps (not shown here). $\Delta I(T_{stress} + T_{interval})/I_{stress}(T_{stress})$ dependence on $T_{interval}$ is shown in Figure 4. It can be seen that $\Delta I(T_{stress} + T_{interval})/I_{stress}(T_{stress})$ increases and then saturates as $T_{interval}$ increases. This suggests that extra active traps contributing to SILC are created after CCS [8].

We analyzed the time evolution of $\Delta I(T_{stress}+T_{interval})$. We assumed that initial traps created by CCS have a certain, large, internal energy and that the energy is dissipated as structural relaxation occurs around the initial defects. Thus extra trap creation should stop when the internal energy of the initial defects falls below the threshold value of trap creation; in other words, $\Delta I(T_{stress} + T_{interval})$ should saturate. Since the structural relaxation of the defect region induces additional traps surrounding the initial defect region, $\Delta I(T_{stress}+T_{interval})$ stemming from the extra traps can be characterized by the effective volume of structural relaxation region ($V(t)$).

3.3. Possible Physical Models. In this paper, we reconsider the above empirical understanding of the degradation. Under electrical stress, some of the electrons injected from the electrode lose energy through inelastic scattering processes. Molecules accumulate energy by these events (detailed in the appendix). After the electrical stress is stopped, molecules having any extra energy transfer the energy to surrounding molecules, which yields electronic traps at the surrounding molecules.

It can be anticipated that the differential equation describing this phenomenon is given by

$$\alpha_1 \frac{dV(t)}{dt} = E_{ta} - E_{sc} N_t V(t), \quad (1)$$

where $V(t)$ is the effective volume enclosing the created traps (cm^3 in unit), α_1 is the energy per volume accumulated at the specific molecule by the electrical stress integration (eVsec/cm^3 in unit) (see appendix), E_{ta} is the initial total

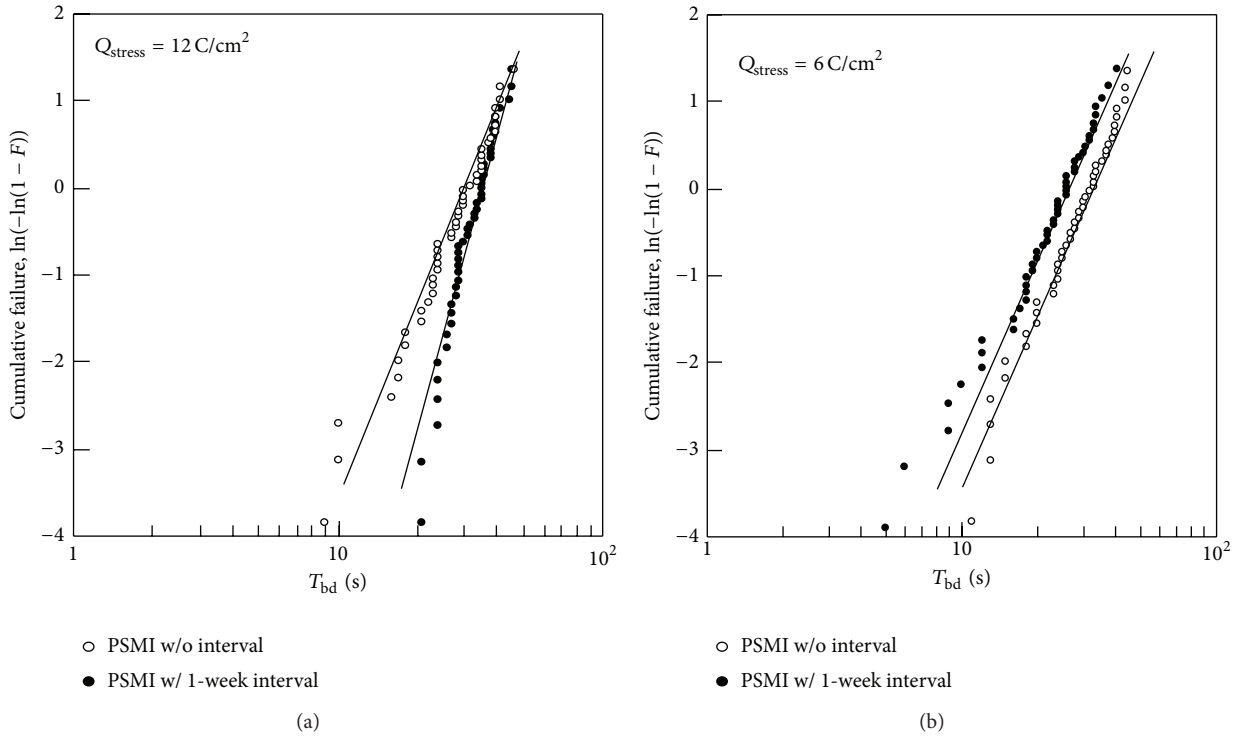

FIGURE 3: Distributions of T_{bd} for various PSMI conditions. (a) T_{bd} distribution for Q_{stress} of 12 C/cm^2. Open circles show the T_{bd} distribution for PSMI without interval. Closed circles show the T_{bd} distribution for *multiple PSMI experiments* with the interval of a week. (b) T_{bd} distribution for Q_{stress} of 6 C/cm^2. Open circles show the T_{bd} distribution for PSMI without interval. Closed circles show the T_{bd} distribution for *multiple PSMI experiments* with the interval of a week.

energy accumulated at the molecule by the electrical stress (eV in unit), E_{sc} is the energy dissipated by a single new trap creation (eV in unit), and N_t is the trap density created (cm^{-3} in unit). When it is assumed that $V(t)$ has the initial value of ~0 cm^{-3}, the solution of (1) is obtained as

$$N_t V(t) = \frac{E_{ta}}{E_{sc}} \left\{1 - \exp\left(-\frac{t}{\tau_1}\right)\right\}, \quad (2)$$

$$\tau_1 = \frac{\alpha_1}{N_t E_{sc}}, \quad (3)$$

where τ_1 is the time constant characterizing the saturation of SILC increment. The left-hand side of (2) means the total trap number at time t. Equation (2) indicates that the total trap number saturates as the unstressed period ($T_{interval}$) increases. Assuming that the increment of SILC component ($\Delta I(T_{stress} + T_{interval})/I(T_{stress})$) is proportional to $V(t)$ according to the consideration described before (1), calculation results are shown by lines in Figure 4 together with measured results, where the parameters of best fit are used. For Figure 4 it is assumed that

$$\frac{\Delta I\left(T_{stress} + T_{interval}\right)}{I\left(T_{stress}\right)} = C_1 \left\{1 - \exp\left(-\frac{t}{\tau_1}\right)\right\}, \quad (4)$$

where C_1 is a constant. Calculated results successfully reproduce the increment in SILC component ($\Delta I(T_{stress} + T_{interval})/I(T_{stress})$) in the early stage of the time evolution; the early stage suggests that the reaction process is determined by just the time constant (τ_1); consider $\tau_1 = 1 \times 10^5$ sec for Q_{stress} = 12 C/cm^2 and $\tau_1 = 2 \times 10^5$ sec for Q_{stress} = 6 C/cm^2. The time constant means the averaged "total time" in which each trap is entirely created by structural relaxation. However, the calculated curves do not reproduce all of the measured results, so a second process must be posited. In the previous paper [8], the author demonstrated that the stage of medium degradation is ruled by the diffusion processes of molecule species H_2 and H_2O [8]. Therefore, it can be considered that $\Delta I(T_{stress} + T_{interval})/I(T_{stress})$ is not proportional to just extra trap density and $T_{interval}$ as shown in Figure 4. This means that the extra active trap creation process must involve another differential equation because the degradation mechanism is not a simple reaction process.

We investigated how to reproduce the measured results by applying an analytical model. Following the previous consideration, it is anticipated that the normalized degradation of SILC is proportional to the normalized conductance degradation as shown by [5]

$$\frac{\Delta I\left(T_{stress} + T_{interval}\right)}{I\left(T_{stress}\right)} \propto \frac{\Delta\sigma_{trap}}{\sigma_{trap}}, \quad (5)$$

where σ_{trap} is the conductance of the poststressed SiO_2 film and $\Delta\sigma_{trap}$ is the incremental conductance of the film. When the effective radius of the initial defect is given as r, the defect volume is given by $V(r) = (4/3)\pi r^3$. It follows that the

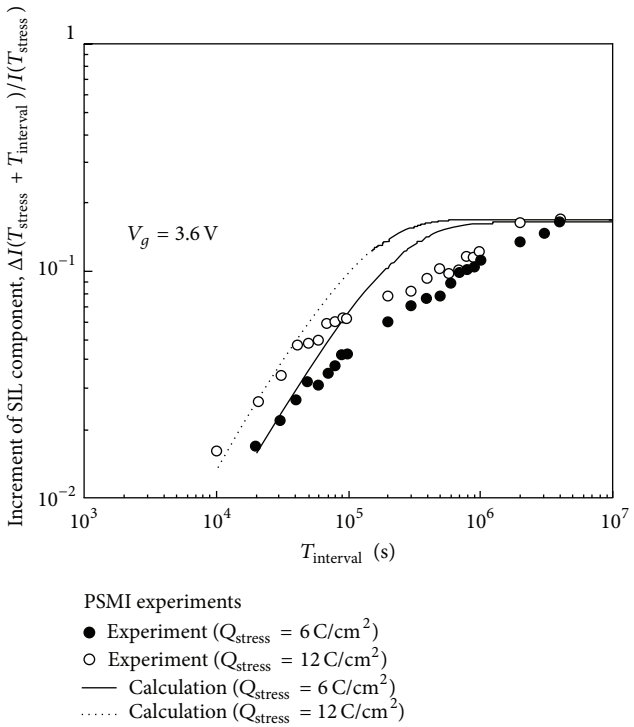

FIGURE 4: Time evolution of gate current ($\Delta I(T_{stress} + T_{interval})/I_{stress}(T_{stress})$) after *a single* stress application. Symbols are measured results, and lines are the results calculated using (2). The CCS condition is 500 mA/cm^2 in all experiments. Q_{stress} is 6 C/cm^2 or 12 C/cm^2.

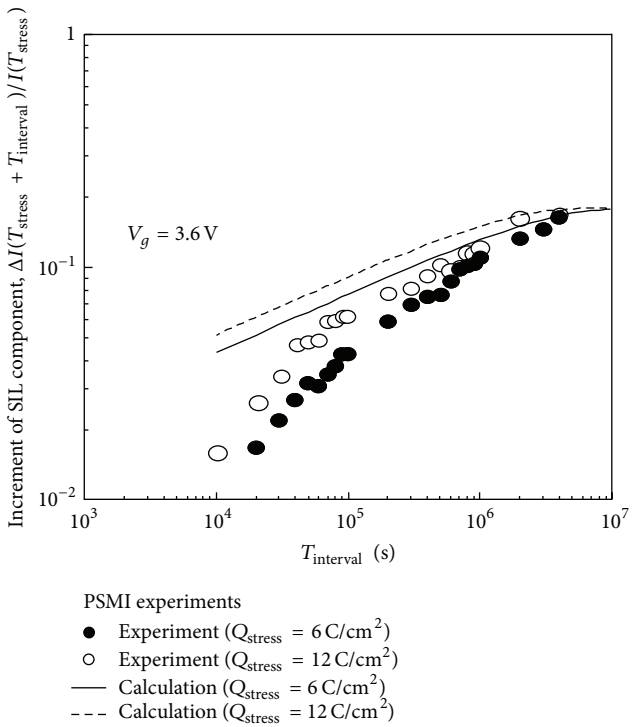

FIGURE 5: Time evolution of gate current ($\Delta I(T_{stress} + T_{interval})/I_{stress}(T_{stress})$) after *a single* stress application. The CCS condition is 500 mA/cm^2 in all experiments. Q_{stress} is 6 C/cm^2 or 12 C/cm^2. Symbols are measured results, and lines are the results calculated using (8). The characteristic time constant (τ_2) is 3.0×10^6 sec for Q_{stress} = 6 C/cm^2 and 1.5×10^6 sec for Q_{stress} = 12 C/cm^2.

assumption that the incremental SILC is ruled primarily by the in-depth expansion of the extra trap region [20] yields the following relation:

$$\frac{\Delta\sigma_{trap}}{\sigma_{trap}} \propto \sqrt[3]{\frac{dV(r(t))}{dr(t)}} \propto V(r(t))^{2/9}. \quad (6)$$

On the other hand, the assumption that the incremental SILC is ruled primarily by the in-plane lateral expansion [21] of the extra trap region yields the following relation:

$$\frac{\Delta\sigma_{trap}}{\sigma_{trap}} \propto V(r(t))^{4/9}. \quad (7)$$

(i) Possibility of One-Dimensional Percolation Process of Trap Creation. Combining (2), (5), and (6), we have

$$\frac{\Delta I(T_{stress} + T_{interval})}{I(T_{stress})} = C_2 \left\{1 - \exp\left(-\frac{t}{\tau_2}\right)\right\}^{2/9}, \quad (8)$$

$$\tau_2 = \frac{\alpha_2}{N_t E_{sc}}, \quad (9)$$

where C_2 is a constant, τ_2 is the time constant characterizing the saturation of the incremental SILC, and α_2 is the energy per volume accumulated by the electrical stress integration (eVsec/cm^3 in unit) assuming the one-dimensional percolation process of trap creation.

Calculated curves are shown in Figure 5 together with the measured results; the value of τ_2 is about 3×10^6 sec for the injected charge of 6 C/cm^2 and about 1.5×10^6 sec for the injected charge of 12 C/cm^2. The proposed model roughly traces the second stage demonstrated by all measured results. As a consequence, the relation $\Delta I(T_{stress} + T_{interval})/I_{stress}(T_{stress}) \sim T_{interval}{}^{1/4}$ can be used for $\tau_2/10 < T_{interval} < \tau_2$. This suggests that the increase in SILC is related to the one-dimensional percolation process of trap creation [20]. However, if we attempt to assume that the second stage is primarily ruled by a mechanism independent of that of the first stage, we must note that (8) does not comprehensively explain all measured results by itself. In this paper, we assume that the second stage is composed of two different mechanisms (separate from the mechanism appearing in the first stage). Therefore, we can consider that the second stage of degradation is primarily ruled by the two-dimensional expansion of extra trap creation.

(ii) Possibility of In-Plane Diffusion Process of Trap Creation [21]. Combining (2), (5), and (7) yields

$$\frac{\Delta I(T_{stress} + T_{interval})}{I(T_{stress})} = C_3 \left\{1 - \exp\left(-\frac{t}{\tau_3}\right)\right\}^{4/9}, \quad (10)$$

$$\tau_3 = \frac{\alpha_3}{N_t E_{sc}}, \quad (11)$$

where C_3 is a constant, τ_3 is the time constant characterizing the saturation of the incremental SILC, and α_3 is the energy per volume accumulated by the electrical stress integration (eVsec/cm^3 in unit) assuming the in-plane diffusion process of trap creation.

In order to examine whether the two mechanisms modeled by (2) and (10) rule the process, the following equation is assumed:

$$\frac{\Delta I\left(T_{\text{stress}}+T_{\text{interval}}\right)}{I\left(T_{\text{stress}}\right)} \propto 1\cdot\left(\frac{1}{\left[\Delta I(T_{\text{stress}}+T_{\text{interval}})/I(T_{\text{stress}})\right]_{(4)}}+\frac{1}{\left[\Delta I(T_{\text{stress}}+T_{\text{interval}})/I(T_{\text{stress}})\right]_{(10)}}\right)^{-1} = \frac{C_1C_3\left\{1-\exp\left(-t/\tau_1\right)\right\}\left\{1-\exp\left(-t/\tau_3\right)\right\}^{4/9}}{C_1\left\{1-\exp\left(-t/\tau_1\right)\right\}+C_3\left\{1-\exp\left(-t/\tau_3\right)\right\}^{4/9}}. \quad (12)$$

Here, it is assumed that $C_1 = C_3 = 1$ for simplicity. Calculated curves are shown in Figure 6 together with measured results. The value of τ_3 is about 3×10^6 sec for the injected charge of 6 C/cm^2 and about 1.5×10^6 sec for the injected charge of 12 C/cm^2. The proposed model (12) reproduces the early-to-final stage of all measured results. As a consequence, the relation $\Delta I(T_{\text{stress}} + T_{\text{interval}})/I_{\text{stress}}(T_{\text{stress}}) \sim {T_{\text{interval}}}^{1/2}$ can be used to explain the primary mechanism of the second stage. This strongly suggests that the increase in SILC is related to the two-dimensional percolation process of extra trap creation, in other words, the diffusion process of some specific material as suggested in [8, 22].

3.4. Extraction of Physical Parameters. (i) Using (A.2) and (A.3), we can estimate the values of E_{ta} and α_i. They are given as

$$E_{ta} = 5.5 \times 10^{-14}\ [\text{J}]\ (\text{for } Q_{\text{stress}} = 6\ \text{C/cm}^2);$$
$$E_{ta} = 1.1 \times 10^{-13}\ [\text{J}]\ (\text{for } Q_{\text{stress}} = 12\ \text{C/cm}^2);$$
$$\alpha_i = 5.2 \times 10^9\ [\text{Js/cm}^3]\ (\text{for } Q_{\text{stress}} = 6\ \text{C/cm}^2);$$
$$\alpha_i = 2.1 \times 10^{10}\ [\text{Js/cm}^3]\ (\text{for } Q_{\text{stress}} = 12\ \text{C/cm}^2).$$

Although the estimated values of E_{ta} seem large, they lie in an acceptable range when we estimate the number of electrons scattered by atoms under electrical stress. Values of α_i suggest that the energy accumulated by one-second of electrical stress is ~10^{-13} J/atom, and we can consider that they are also in a reasonable range.

Next we estimate the trap density created (N_t) using (A.4). When we use the values of τ_3 extracted from experimental results (3×10^6 s for $Q_{\text{stress}} = 6$ C/cm^2 and 1.5×10^6 s for $Q_{\text{stress}} = 12$ C/cm^2), we have

$$N_t E_{\text{sc}} = 1.7 \times 10^3\ [\text{J/cm}^3]\ (\text{for } Q_{\text{stress}} = 6\ \text{C/cm}^2),$$
$$N_t E_{\text{sc}} = 1.4 \times 10^4\ [\text{J/cm}^3]\ (\text{for } Q_{\text{stress}} = 12\ \text{C/cm}^2).$$

Using estimated E_{ta} values, we have

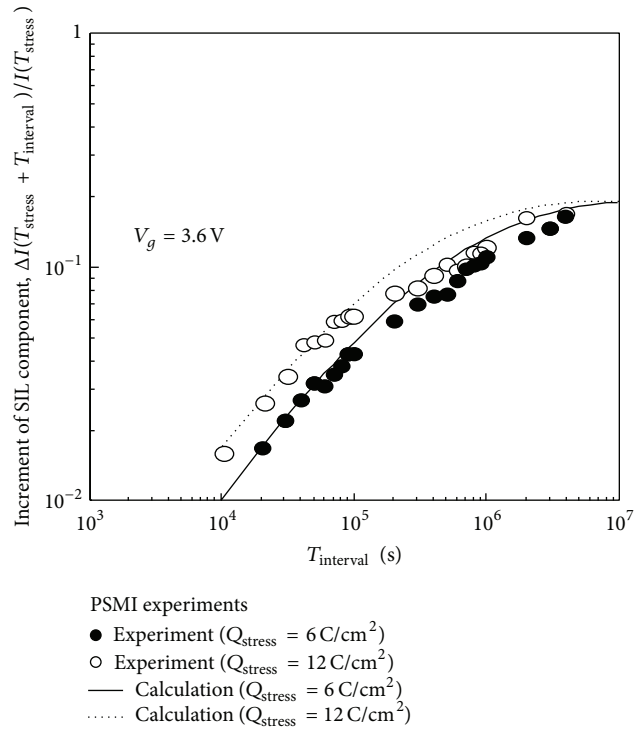

FIGURE 6: Time evolution of gate current ($\Delta I(T_{\text{stress}} + T_{\text{interval}})/I_{\text{stress}}(T_{\text{stress}})$) after *a single* stress application. The CCS condition is 500 mA/cm^2 in all experiments. Q_{stress} is 6 C/cm^2 or 12 C/cm^2. Symbols are measured results, and lines are the results calculated using (12). The characteristic time constant (τ_3) is 3.0×10^6 sec for $Q_{\text{stress}} = 6$ C/cm^2 and 1.5×10^6 sec for $Q_{\text{stress}} = 12$ C/cm^2.

$$N_t > 3.1 \times 10^{16}\ [/\text{cm}^3]\ (\text{for } Q_{\text{stress}} = 6\ \text{C/cm}^2),$$
$$N_t > 1.3 \times 10^{17}\ [/\text{cm}^3]\ (\text{for } Q_{\text{stress}} = 12\ \text{C/cm}^2).$$

These values mean that the density of traps created is much larger than 10^{10} cm^{-2}. These values of physical parameters are acceptable based on various SILC-related experimental results in past articles [1–3, 5–8, 17, 20–23].

(ii) When it is assumed that some material is diffusing within the film, the diffusion constant (D) can be estimated by r_v^2/τ_3, where r_v is the radius of the in-plane expansion of the extra trap creation. This yields the following important relation between the diffusion constant (D) and the trap density (N_t):

$$D = \frac{2r_v^2}{\tau_3}. \quad (13a)$$

We have already found that the expansion of extra trap creation is three-dimensional [23]; this suggests $r_v \sim T_{\text{ox}}$, where T_{ox} is SiO_2 film thickness. Thus, we have

$$D = \frac{2T_{\text{ox}}^2}{\tau_3}. \quad (13b)$$

Since $\tau_3 = 1.5 \times 10^6$ s to 3.0×10^6 s, the estimated diffusion constant of damaged SiO_2 film examined here has a value

of 3.6×10^{-19} to 1.8×10^{-19} cm^2/s. In unstressed SiO_2 film, it is known that the diffusion constant of H_2O molecules is about 6.4×10^{-20} cm^2/s [22]. As suggested in [8], the diffusion constant of H_2O molecules in a poststressed SiO_2 film in a certain unstressed interval should be about ten times larger than that in an unstressed SiO_2 film [8]. Therefore, the analysis proposed here is reasonable and very useful for extracting several parameters from measured results.

According to related studies [8, 22], H_2O molecules are the most likely material at room temperature. It is already known that many neutral traps are created just after electron injection, so it is anticipated that those neutral traps are activated by being terminated with H or OH species; that is, O–Si–H and HO–Si–O structures are created [8]. From this discussion, it can be considered that all traps are created as neutral traps just after stress termination and that H_2O molecules activate the neutral traps by bonding with them [8]. We consider that Figure 6 demonstrates the veracity of this simplified model in assuming the diffusion of H_2O molecules through the film at room temperature.

In the case of the resistive transition phenomenon, the electric-field-induced diffusion of oxygen ions is usually assumed [8, 24, 25]. The above consideration strongly suggests that the oxygen diffusion is supported by hydrogen molecules [8] and simple ionic transport.

4. Summary

In this paper, a poststress time evolution model for sub-10-nm thick SiO_2 films was proposed for degradation prediction and the extraction of trap-related parameters. The model is based on the fact that the degradation in thin SiO_2 films continues within the unstressed interval. The phenomenon was represented by an analytical expression that reflects the fact that SiO_2 film degradation is more likely to occur in the presence of water molecules. The proposed model successfully predicted the increase in the diffusion constant of water molecules, and it also successfully reproduced the measured results. Therefore, the proposed model is useful for the purpose of extracting degradation parameters from measured results.

Appendix

On the Accumulation Energy per Volume around the SiO_2 Molecule

When it is assumed that T_{ox} is the oxide layer thickness, F is the electric field, T_{stress} is the stress time, a_l is the lattice constant, I_{stress} is the stress current, and S_G is the gate electrode area, we have

$$E_{ta} = \frac{I_{stress}}{eS_G} \times a_l^2 \times eFT_{ox} \times T_{stress}. \quad (A.1)$$

On the other hand, E_{ta} relates the total energy accumulated at the specific molecule (α_1, α_2, or α_3) as

$$E_{ta} = \alpha_i \times \frac{a_l^3}{T_{stress}}, \quad (i = 1, 2, \text{or } 3). \quad (A.2)$$

Combining (A.1) and (A.2), we have

$$\alpha_i = \frac{I_{stress} F T_{ox} T_{stress}^2}{a_l S_G}. \quad (A.3)$$

From (3), (9), and (11), we have

$$\tau_i = \frac{I_{stress} F T_{ox} T_{stress}^2}{N_t E_{sc} a_l S_G}. \quad (A.4)$$

Conflict of Interests

The author declares that there is no conflict of interests regarding the publication of this paper.

Acknowledgment

The author expresses his thanks to Mr. A. Masuo, graduate student (presently, Panasonic Corp., Japan), for his technical support in experiments.

References

[1] K. Sakakibara, N. Ajika, K. Eikyu, K. Ishikawa, and H. Miyoshi, "A quantitative analysis of time-decay reproducible stress-induced leakage current in SiO_2 films," *IEEE Transactions on Electron Devices*, vol. 44, no. 6, pp. 1002–1008, 1997.

[2] S.-I. Takagi, N. Yasuda, and A. Toriumi, "A new I-V model for stress-induced leakage current including inelastic tunneling," *IEEE Transactions on Electron Devices*, vol. 46, no. 2, pp. 348–354, 1999.

[3] S. Satoh, G. Hemink, K. Hatakeyama, and S. Aritome, "Stress-induced leakage current of tunnel oxide derived from flash memory read-disturb characteristics," *IEEE Transactions on Electron Devices*, vol. 45, no. 2, pp. 482–486, 1998.

[4] Semiconductor Industry Association, *International Technology Roadmap for Semiconductors*, Semiconductor Industry Association, 2010.

[5] D. J. Dimaria and E. Cartier, "Mechanism for stress-induced leakage currents in thin silicon dioxide films," *Journal of Applied Physics*, vol. 78, no. 6, pp. 3883–3894, 1995.

[6] R. Degraeve, G. Groeseneken, R. Bellens et al., "New insights in the relation between electron trap generation and the statistical properties of oxide breakdown," *IEEE Transactions on Electron Devices*, vol. 45, no. 4, pp. 904–911, 1998.

[7] S. Lombardo, J. H. Stathis, B. P. Linder, K. L. Pey, F. Palumbo, and C. H. Tung, "Dielectric breakdown mechanisms in gate oxides," *Journal of Applied Physics*, vol. 98, no. 12, Article ID 121301, 2005.

[8] Y. Omura, "Possible model of degradation mechanism that increments the gate current (nonbiased interval) after constant-current stress," *Journal of Applied Physics*, vol. 102, no. 3, Article ID 033710, pp. 1–7, 2007.

[9] N. Raghavan, K. L. Pey, W. Liu, X. Wu, X. Li, and M. Bosman, "Evidence for compliance controlled oxygen vacancy and metal filament based resistive switching mechanisms in RRAM," *Microelectronic Engineering*, vol. 88, no. 7, pp. 1124–1128, 2011.

[10] Y.-F. Chang, P.-Y. Chen, B. Fowler et al., "Understanding the resistive switching characteristics and mechanism in active SiOx-based resistive switching memory," *Journal of Applied Physics*, vol. 112, no. 12, Article ID 123702, 2012.

[11] Y. Omura and Y. Kondo, "Impact-ionization-based resistive transition model for thin TiO_2 films," *Journal of Applied Physics*, vol. 114, no. 4, Article ID 043712, 2013.

[12] T. W. Hickmott, "Low-frequency negative resistance in thin anodic oxide films," *Journal of Applied Physics*, vol. 33, no. 9, pp. 2669–2682, 1962.

[13] R. Waser and M. Aono, "Nanoionics-based resistive switching memories," *Nature Materials*, vol. 6, no. 11, pp. 833–840, 2007.

[14] Y. Omura and H. Nakatsuji, "Distinctive observation of valence-band electron direct-tunneling current in a nanometer-thick silicon oxide film on monocrystalline silicon," *Applied Physics Letters*, vol. 75, no. 4, pp. 513–515, 1999.

[15] K. Komiya and Y. Omura, "Spectroscopic characterization of stress-induced leakage current in sub 5-nm-thick silicon oxide film," *Journal of Applied Physics*, vol. 92, no. 5, pp. 2593–2601, 2002.

[16] Y. Fong, I. C. Chen, S. Holland, J. Lee, and C. Hu, "Dynamic stressing of thin oxides," in *Proceedings of the IEEE International Electron Devices Meeting Technical Digest (IEDM '86)*, pp. 664–667, IEEE, 1986.

[17] B. Wang, J. S. Suehle, E. M. Vogel, and J. B. Bernstein, "Time-dependent breakdown of Ultra-thin SiO_2 gate dielectrics under pulsed biased stress," *IEEE Electron Device Letters*, vol. 22, no. 5, pp. 224–226, 2001.

[18] P. Fiorenza, W. Polspoel, and W. Vandervorst, "Conductive atomic force microscopy studies of thin SiO_2 layer degradation," *Applied Physics Letters*, vol. 88, no. 22, Article ID 222104, 2006.

[19] W. Polspoel, P. Favia, J. Mody, H. Bender, and W. Vandervorst, "Physical degradation of gate dielectrics induced by local electrical stress using conductive atomic force microscopy," *Journal of Applied Physics*, vol. 106, no. 2, Article ID 024101, 2009.

[20] H. Satake and A. Toriumi, "SiO_2 dielectric breakdown mechanism studied by the post-breakdown resistance statistics," *Semiconductor Science and Technology*, vol. 15, no. 5, pp. 471–477, 2000.

[21] S. S. Sombra, U. M. S. Costa, V. N. Freire, E. A. de Vasconcelos, and E. F. Da Silva Jr., "The role of multiple damaged layers at the Si/SiO_2 interface on the dielectric breakdown of MOS capacitors," *Applied Surface Science*, vol. 190, no. 1–4, pp. 35–38, 2002.

[22] G. van den Bosch, G. Groeseneken, and H. E. Maes, "Direct and post-injection oxide and interface trap generation resulting from low-temperature hot-electron injection," *Journal of Applied Physics*, vol. 74, no. 9, pp. 5582–5586, 1993.

[23] A. Masuo, K. Komiya, and Y. Omura, "Extra-trap creation within unstressed interval under cyclic application of constant-current stress to thin SiO_2 films," in *Proceedings of the Extended Abstracts of International Workshop on Gate Insulator (IWGI '01)*, pp. 114–115, Tokyo, Japan, November 2001.

[24] C. Vallée, P. Gonon, C. Jorel, F. El Kamel, M. Mougenot, and V. Jousseaume, "High κ for MIM and RRAM applications: Impact of the metallic electrode and oxygen vacancies," *Microelectronic Engineering*, vol. 86, no. 7–9, pp. 1774–1776, 2009.

[25] G. Bersuker, D. C. Gilmer, D. Veksler et al., "Metal oxide RRAM switching mechanism based on conductive filament microscopic properties," in *Proceedings of the IEEE International Electron Devices Meeting (IEDM '10)*, pp. 19.6.1–19.6.4, San Francisco, Calif, USA, December 2010.